

# Direct determination of the crystallographic orientation of graphene edges by atomic resolution imaging

S. Neubeck,<sup>1</sup> Y. M. You,<sup>2</sup> Z. H. Ni,<sup>1,2</sup> P. Blake,<sup>3</sup> Z. X. Shen,<sup>2</sup> A. K. Geim,<sup>3</sup> and K. S. Novoselov<sup>1,a)</sup>

<sup>1</sup>*School of Physics and Astronomy, University of Manchester, Manchester M13 9PL, United Kingdom*

<sup>2</sup>*Division of Physics and Applied Physics School of Physical and Mathematical Sciences, Nanyang Technological University, Singapore 637371*

<sup>3</sup>*Centre for Mesoscience and Nanotechnology, University of Manchester, Manchester M13 9PL, United Kingdom*

(Received 9 May 2010; accepted 4 June 2010; published online 4 August 2010)

In this letter, we show how high-resolution scanning tunneling microscopy (STM) imaging can be used to reveal that certain edges of micromechanically exfoliated single layer graphene crystals on silicon oxide follow either zigzag or armchair orientation. Using the cleavage technique, graphene flakes are obtained that very often show terminating edges seemingly following the crystallographic directions of the underlying honeycomb lattice. Performing atomic resolution STM-imaging on such flakes, we were able to directly prove this assumption. Raman imaging carried out on the same flakes further validated our findings. © 2010 American Institute of Physics.

[doi:10.1063/1.3467468]

Graphene, the monolayer of carbon atoms arranged into a hexagonal lattice, was first isolated in 2004 by using the micromechanical cleavage technique.<sup>1,2</sup> Although a number of other methods for graphene synthesis have been proposed since then (including the reduction in graphene oxide,<sup>3</sup> decomposition of silicon carbide,<sup>4,5</sup> epitaxial growth on nickel and other substrates,<sup>6–9</sup> or direct chemical exfoliation<sup>10,11</sup>) the micromechanical technique (also known as the “Scotch-tape method”) is still the procedure of choice for many researchers. Furthermore, the uniqueness of this procedure is that it reveals the peculiar micromechanical properties of this material, which might be used in obtaining crystallographically oriented graphene samples.

The choice of crystallographic orientation of the graphene flakes might be of crucial importance for the electronic properties of resulting devices.<sup>12–14</sup> Two following problems generally arise: (i) how to determine the crystallographic orientation of a particular graphene crystallite and (ii) how to prepare a device which is oriented exactly along one of those directions. Whenever there are quite a few ways for determination of the orientation,<sup>15–19</sup> preparation of well oriented edges is a tantalizing task.<sup>20</sup>

It has been noted<sup>21</sup> that flakes obtained by the “Scotch-tape method” often exhibit straight edges with the angle between the adjacent ones being a multiple of 30°. An example of such a flake is shown in Fig. 1(a).

Considering the hexagonal symmetry of graphene crystals, it has been suggested that the breaking occurs along the principal crystallographic directions, yielding flakes terminated with either armchair or zigzag edges.<sup>21,22</sup> Previously, Raman measurements have been employed to verify this idea,<sup>17,18</sup> demonstrating a clear difference in the amplitude of the D peak for edges oriented along zigzag and armchair directions. However, Raman measurements require elaborate modeling to explain the finding.

In this letter, we will use high-resolution scanning tunneling microscopy (STM) to prove beyond doubt that edges of graphene crystals are predominantly oriented along crystallographic directions. The main advantage of high-resolution STM compared to the aforementioned techniques is its ability to provide direct real-space images of the graphene crystal lattice with atomic resolution. Additionally, there is no need for having suspended samples in order to carry out STM investigations. Thus, it ultimately enables one to directly determine the crystallographic orientation of a given graphene flake, and hence the orientation of the edges terminating that sample. We also compare the results of the STM study to the Raman measurements.

Single layer graphene flakes were obtained by micromechanical cleavage of natural graphite. Exfoliated graphite flakes were deposited on top of an oxidized silicon wafer (300 nm of SiO<sub>2</sub>), and crystallites of single layer thickness were identified using optical microscopy.<sup>23</sup> For our studies, we used flakes with a significant percentage of edges forming angles which are integer multiples of 30°. Examples of such flakes are shown in Figs. 1(a) and 2(a). Upon selection

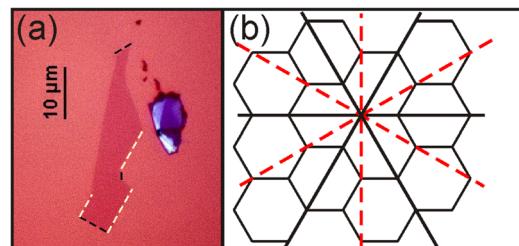


FIG. 1. (Color online) (a) Optical image of a single layer graphene flake prepared by micromechanical cleavage. It can be clearly seen that the edges terminating the graphene crystal follow straight lines up to lengths of several micrometers. Certain edges of this particular flake, oriented relative to each other in integer multiples of 30°, have been highlighted by a dashed line (black and white, for the respective type of edge). (b) Sketch of the honeycomb crystal lattice of graphene. Two distinct crystallographic orientations of a graphene crystal are possible: armchair (solid lines), and zigzag (dashed lines).

<sup>a)</sup>Author to whom correspondence should be addressed. Electronic mail: konstantin.novoselov@manchester.ac.uk.

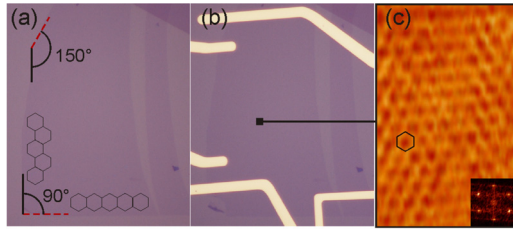


FIG. 2. (Color online) (a) Typical graphene flake obtained by micromechanical cleavage. Two distinct types of edges, rotated against each other in multiples of  $30^\circ$ , are indicated as armchair type (solid lines) and zigzag type (dashed lines). (b) To carry out STM imaging, the flake in (a) was equipped with electrical contacts, and oriented carefully along the scanning direction of the STM-tip. (c) STM constant-height image [ $+0.223$  V and  $(2.8 \pm 0.3)$  nA], showing atomic resolution of the graphene hexagonal lattice. The inset on the lower right shows the Fourier transform of that image, where six well resolved diffraction spots are clearly visible. A single black hexagon is drawn as guide to the eye. Superimposing that hexagon onto the optical image proves the crystallographic orientation of the two indicated edge types.

of appropriate flakes, we used e-beam lithography to define electrical contacts on the flakes (Ti, 5 nm+Au, 40 nm) [Fig. 2(b)].

In order to find out whether the edges of, e.g., the graphene flake shown in Fig. 2(a) follow crystallographic orientations, we carried out high-resolution STM investigations. A Multimode scanning probe microscope with a Nanoscope IIIa controller was employed for conducting the STM experiments. All STM experiments were carried out under ambient conditions. Tunneling tips were made out of mechanically cut  $\text{Pt}_{80}/\text{Ir}_{20}$ -wire. The samples were precisely positioned in our STM, and the scanning direction was carefully aligned with one of the edges. Prior to imaging, the flakes were annealed at  $250^\circ\text{C}$  in a hydrogen/argon-atmosphere,<sup>24</sup> in order to remove resist residuals due to the lithography treatment. After that, the flakes were found to be clean enough to achieve atomic resolution. Figure 2(c) shows an STM image of the graphene flake shown in Fig. 2(a), taken in constant-height mode at a sample bias of 223 mV and a set-point tunneling current of 2.8 nA (the tunneling current varied by a maximum of  $\pm 0.3$  nA between positions on the atoms and interatomic positions). The atomically resolved hexagonal graphene lattice can be clearly seen, which is a clear proof of the monolayer character of this particular sample.<sup>25</sup> The Fourier transform of that image, shown in the inset on the lower right of Fig. 2(c), accordingly shows six well-resolved diffraction peaks. Both the atomically resolved image of the lattice and the Fourier transform image allow us to determine the orientation of the edges of a given graphene flake. This is done by virtually tiling the entire graphene flake under question with the experimentally observed hexagonal unit cell (or equivalently the corresponding Fourier transform). Following this approach for the flake shown in Fig. 2(a), we can identify the vertical edge as being armchair and the horizontal edge as being zigzag.

Additional information about the edges can be obtained from the Raman measurements. Recent results show that it is possible to distinguish between armchair and zigzag orientation by Raman spectroscopy.<sup>17</sup> The disorder-induced Raman feature of graphene (D peak at  $\sim 1350$   $\text{cm}^{-1}$ ) is activated through a double resonance process<sup>26</sup> and is often observed at the edges. This is because the edges act as defects, allow-

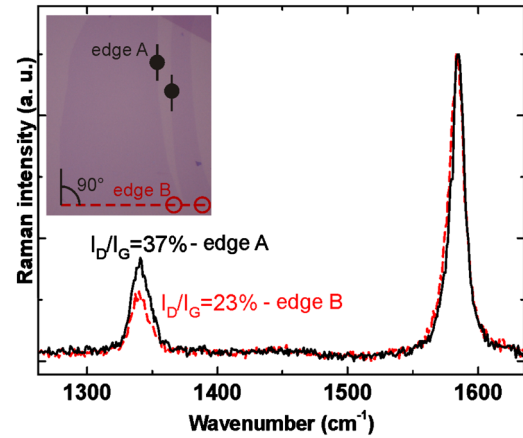


FIG. 3. (Color online) Raman spectra taken from two different edges (optical image shown in the inset on the upper left), labeled edge A (vertical solid line, solid spots) and edge B (horizontal dashed line, open spots), forming an angle of  $90^\circ$ . As graphene has a hexagonal crystal lattice, the two edges are believed to have different chirality. During the measurement, the laser polarization (linear) is oriented parallel to the graphene edge being measured, to maximize the D peak signal (Refs. 17 and 27). The Raman spectra at edge A (solid curve) shows a D-peak intensity of  $\sim 37\%$  compared to the G-peak intensity, while it is only  $\sim 23\%$  for the spectra taken at edge B (dashed curve). Raman spectra from different spots of the two edges gave similar results. This confirms our finding that edge A is armchair, whereas edge B is zigzag.

ing elastic backscattering of electrons to fulfill the double resonance condition.<sup>27</sup> The D peak was reported to be stronger at the armchair edge and weaker at the zigzag edge, due to the momentum conservation (armchair edges can scatter electrons between two nonequivalent Dirac cones, while zigzag edges cannot).<sup>17,27</sup> Raman measurements were carried out using a WITec CRM200 confocal microscopy Raman system with a  $100\times$  objective lens (numerical aperture = 0.95). The excitation laser wavelength is 532 nm. We measured Raman spectra from points A and B, which are two edges forming an angle of  $90^\circ$ , as labeled in the inset (optical image) of Fig. 3.

During the measurement, the laser polarization (linear) is oriented parallel to the graphene edge under investigation, in order to maximize the D peak signal.<sup>17,27</sup> To determine the exact position of the graphene edge, Raman spectra were taken at different positions while scanning the laser spot perpendicularly across the particular edge under question (with a step size of 50 nm). The maximum intensity of the D-band measured under these conditions was taken in order to compare the two different edges. As shown in Fig. 3, at point A, the D peak intensity is  $\sim 37\%$  of that of the G peak, while it is only  $\sim 23\%$  at point B. This suggests that the edge containing point A is armchair while the other edge is zigzag. Raman spectra from different points of the two edges were checked and similar results were obtained. The Raman results confirm the STM results of the graphene crystallographic orientation. Here, we have to clarify that the edges mentioned above are predominantly crystallographic, as perfect zigzag and armchair edges are extremely rare. There are small amounts of armchair sections even on zigzag edges, both on exfoliated single layer graphene<sup>13,28,29</sup> and terraces on bulk graphite,<sup>30</sup> which contribute to the observed D peak at point B.

In conclusion, we have demonstrated the direct determination of the crystallographic orientation of graphene edges

by using high-resolution STM. The obtained atomic resolution images of the graphene crystal lattice have allowed us to unambiguously identify both armchair and zigzag edges of a given graphene flake prepared by mechanical exfoliation. Complementary information has been obtained by Raman spectroscopy, fully justifying our assumption that certain edges on micromechanically exfoliated samples predominantly follow crystallographic orientations of the underlying graphene crystal lattice.

This work was supported by Engineering and Physical Sciences Research Council (U.K.), the Royal Society, the European Research Council, Office of Naval Research (Grant No. N00014-08-1-0277), and Air Force Office of Scientific Research (Grant No. FA8655-08-1-3088). S.N. would like to thank Evonik Stiftung (Germany) for kind financial support. The authors are grateful to Nacional de Grafite for supplying high quality crystals of graphite.

- <sup>1</sup>K. S. Novoselov, A. K. Geim, S. V. Morozov, D. Jiang, Y. Zhang, S. V. Dubonos, I. V. Grigorieva, and A. A. Firsov, *Science* **306**, 666 (2004).
- <sup>2</sup>K. S. Novoselov, D. Jiang, F. Schedin, T. J. Booth, V. V. Khotkevich, S. V. Morozov, and A. K. Geim, *Proc. Natl. Acad. Sci. U.S.A.* **102**, 10451 (2005).
- <sup>3</sup>S. Stankovich, D. A. Dikin, G. H. B. Dommett, K. M. Kohlhaas, E. J. Zimney, E. A. Stach, R. D. Piner, S. T. Nguyen, and R. S. Ruoff, *Nature (London)* **442**, 282 (2006).
- <sup>4</sup>A. J. Van Bommel, J. E. Crombeen, and A. van Tooren, *Surf. Sci.* **48**, 463 (1975).
- <sup>5</sup>C. Berger, Z. Song, T. Li, X. Li, A. Y. Ogbazghi, R. Feng, Z. Dai, A. N. Marchenkov, E. H. Conrad, P. N. First, and W. A. de Heer, *J. Phys. Chem. B* **108**, 19912 (2004).
- <sup>6</sup>C. Oshima and A. Nagashima, *J. Phys.: Condens. Matter* **9**, 1 (1997).
- <sup>7</sup>A. Reina, X. Jia, J. Ho, D. Nezich, H. Son, V. Bulovic, M. S. Dresselhaus, and J. Kong, *Nano Lett.* **9**, 30 (2009).
- <sup>8</sup>K. S. Kim, Y. Zhao, H. Jang, S. Y. Lee, J. M. Kim, K. S. Kim J.-H. Ahn, P. Kim, J.-Y. Choi, and B. H. Hong, *Nature (London)* **457**, 706 (2009).
- <sup>9</sup>X. Li, W. Cai, J. An, S. Kim, J. Nah, D. Yang, R. Piner, A. Velamakanni, I. Jung, E. Tutuc, S. K. Banerjee, L. Colombo, and R. S. Ruoff, *Science* **324**, 1312 (2009).
- <sup>10</sup>P. Blake, P. D. Brimicombe, R. R. Nair, T. J. Booth, D. Jiang, F. Schedin, L. A. Ponomarenko, S. V. Morozov, H. F. Gleeson, E. W. Hill, A. K. Geim, and K. S. Novoselov, *Nano Lett.* **8**, 1704 (2008).
- <sup>11</sup>Y. Hernandez, V. Nicolosi, M. A. Lotya, F. M. Blighe, Z. Sun, S. Dei, I. T. McGovern, B. Holland, M. Byrne, Y. K. Gun'ko, J. J. Boland, P. Niraj, G. Duesberg, S. Krishnamurthy, R. Goodhue, J. Hutchison, V. Scardaci, A. C. Ferrari, and J. N. Coleman, *Nat. Nanotechnol.* **3**, 563 (2008).
- <sup>12</sup>N. M. R. Peres, A. H. Castro Neto, and F. Guinea, *Phys. Rev. B* **73**, 195411 (2006).
- <sup>13</sup>L. Yang, C. H. Park, Y. W. Son, M. L. Cohen, and S. G. Louie, *Phys. Rev. Lett.* **99**, 186801 (2007).
- <sup>14</sup>Y.-W. Son, M. L. Cohen, and S. G. Louie, *Nature (London)* **444**, 347 (2006).
- <sup>15</sup>K. A. Ritter and J. W. Lyding, *Nature Mater.* **8**, 235 (2009).
- <sup>16</sup>Ç. Ö. Girit, J. C. Meyer, R. Erni, M. D. Rossell, C. Kisielowski, L. Yang, C.-H. Park, M. F. Crommie, M. L. Cohen, S. G. Louie, and A. Zettl, *Science* **323**, 1705 (2009).
- <sup>17</sup>Y. M. You, Z. H. Ni, T. Yu, and Z. X. Shen, *Appl. Phys. Lett.* **93**, 163112 (2008).
- <sup>18</sup>C. Casiraghi, A. Hartschuh, H. Quian, S. Piscanec, C. Georgi, A. Fasoli, K. S. Novoselov, D. M. Basko, and A. C. Ferrari, *Nano Lett.* **9**, 1433 (2009).
- <sup>19</sup>T. M. G. Mohiuddin, A. Lombardo, R. R. Nair, A. Bonetti, G. Savini, R. Jalil, N. Bonini, D. M. Basko, C. Galiotis, N. Marzari, K. S. Novoselov, A. K. Geim, and A. C. Ferrari, *Phys. Rev. B* **79**, 205433 (2009).
- <sup>20</sup>X. Jia, M. Hofmann, V. Meunier, B. G. Sumpter, J. Campos-Delgado, J. M. Romo-Herrera, H. Son, Y.-P. Hsieh, A. Reina, J. Kong, M. Terrones, and M. S. Dresselhaus, *Science* **323**, 1701 (2009).
- <sup>21</sup>A. K. Geim and K. S. Novoselov, *Nature Mater.* **6**, 183 (2007).
- <sup>22</sup>D. Sen, K. S. Novoselov, P. Reis, and M. J. Buehler, *Small* **6**, 1108 (2010).
- <sup>23</sup>P. Blake, E. W. Hill, A. H. Castro Neto, K. S. Novoselov, D. Jiang, R. Yang, T. J. Booth, and A. K. Geim, *Appl. Phys. Lett.* **91**, 063124 (2007).
- <sup>24</sup>M. Ishigami, J. H. Chen, W. G. Cullen, M. S. Fuhrer, and E. D. Williams, *Nano Lett.* **7**, 1643 (2007).
- <sup>25</sup>E. Stolyarova, K. T. Rim, S. Ryu, J. Maultzsch, P. Kim, L. E. Brus, T. F. Heinz, M. S. Hybertsen, and G. W. Flynn, *Proc. Natl. Acad. Sci. U.S.A.* **104**, 9209 (2007).
- <sup>26</sup>C. Thomsen and S. Reich, *Phys. Rev. Lett.* **85**, 5214 (2000).
- <sup>27</sup>L. G. Cançado, M. A. Pimenta, B. R. A. Neves, M. S. S. Dantas, and A. Jorio, *Phys. Rev. Lett.* **93**, 247401 (2004).
- <sup>28</sup>Z. Liu, K. Suenaga, P. J. F. Harris, and S. Ijima, *Phys. Rev. Lett.* **102**, 015501 (2009).
- <sup>29</sup>Q. Yu, J. Lian, S. Siriponglert, H. Li, Y. P. Chen, and S.-S. Pei, *Appl. Phys. Lett.* **93**, 113103 (2008).
- <sup>30</sup>Y. Niimi, T. Matsui, H. Kambara, K. Tagami, M. Tsukuda, and H. Fukuyama, *Phys. Rev. B* **73**, 085421 (2006).